SPANDIDOS PUBLICATIONS

ONCOLOGY LETTERS 16: 1689-1695, 2018

Functional cardiac Na^+ channels are expressed in human melanoma cells

AN XIE[1,2], BENJAMIN GALLANT[3], HAO GUO[4], ALFREDO GONZALEZ[3], MATTHEW CLARK[3], AUDREY MADIGAN[3], FENG FENG[2], HONG-DUO CHEN[4], YALI CUI[5], SAMUEL C. DUDLEY JR.[1,2] and YINSHENG WAN[3]

[1]Lifespan Cardiovascular Institute, The Warren Alpert School of Medicine of Brown University and The Providence Veterans Administration Medical Center, Providence, RI 02903; [2]Department of Medicine, Lillehei Heart Institute, University of Minnesota, Minneapolis, MN 55455; [3]Department of Biology, Providence College, Providence, RI 02918, USA; [4]Department of Dermatology, No. 1 Hospital of China Medical University, Shenyang 110001; [5]College of Life Science, Northwest University, Xi'an, Shaanxi 710069, P.R. China

Received January 8, 2018; Accepted April 26, 2018

DOI: 10.3892/ol.2018.8865

Abstract. Resting membrane potential (RMP) and intracellular Ca^{2+} concentration [$(Ca^{2+})_i$] are involved in tumorigenesis and metastasis. The present study investigated whether functional cardiac Na^+ channels are expressed in human melanoma cells (WM 266-4) and its nonmalignant human melanocytes (HMC), as well as whether they participate in RMP maintenance and Ca^{2+} homeostasis. Confocal microscopy and western blot analysis were used to detect Na^+ channels. The patch-clamp technique was employed to record Na^+ currents and action potentials. Cytoplasmic Ca^{2+} was measured by loading Fluo-4. Cardiac ($Na_v1.5$) Na^+ channels were expressed in HMCs and WM 266-4 cells. Tetrodotoxin (TTX) dose-dependently blocked Na^+ currents in WM 266-4 while HMCs had no Na^+ currents. Ultraviolet light induced similar action potentials in HMCs and WM 266-4 cells, which were abolished by transient receptor potential A1 channel-specific blocker, HC-030031. Compared with HMCs, RMP was substantially depolarized in WM 266-4. TTX hyperpolarized RMP in WM 266-4 cells at a concentration of 30 μM, which facilitated Ca^{2+} influx. Compared with HMCs, $(Ca^{2+})_i$ was significantly higher in WM 266-4 cells and was elevated by 30 μM TTX. Collectively, Cardiac Na^+ channels depolarize RMP and inhibit Ca^{2+} uptake in melanoma cells possibly contributing to tumorigenesis and metastasis. Na^+ channel agonists may be developed to treat melanoma such as WM 266-4.

Correspondence to: Progessor Yinsheng Wan, Department of Biology, Providence College, 1 Cunningham Square, Providence, RI 02918, USA
E-mail: yswan@providence.edu

Key words: melanoma, Na^+ channel, membrane potential

Introduction

Melanoma cells are transformed melanocytes of neural crest origin. The aggressiveness and metastatic potential of melanoma cells have been intensively studied, and yet the molecular and cellular mechanisms through which melanoma cells behave aberrantly remain to be elucidated. Existing data have shown that human melanocytes (HMC) and melanoma cells have Ca^{2+} channels, neural Na^+ channels, Cl^- channels and K^+ channel (1-3). The activities of those channels have been suggested to be associated with tumorigenesis and metastasis.

Studies have shown that K^+ channels blockers induce a dose-dependent membrane depolarization, which leads to the reduction of the driving force for the influx of Ca^{2+} (4,5). The intracellular Ca^{2+} concentration [$(Ca^{2+})_i$] is related to cell proliferation because transition from G1 to S during mitosis depends on an increase of $[Ca^{2+}]_i$ in mammalian cells (6). Thus, blocking K^+ channels may reduce $[Ca^{2+}]_i$ and attenuate tumorigenesis and metastasis.

Both HMCs and melanoma cells express Cav1 and Cav2 channels. Cav3 and T-type Ca^{2+} channels are only expressed in melanoma cells and mediate constitutively Ca^{2+} influx (7). Ca^{2+} channels directly affect Ca^{2+} handling. Previous reports have also demonstrated that another Ca^{2+} channel named as the calcium release-activated channel (CRAC) is present in 4 types of melanoma (1), although the function of those channels is unknown.

The cardiac Na^+ channel, $Na_v1.5$, has been found in human breast cancer cells and human colon cancer cells. This channel possibly provides favorable conditions for proteolytic activity of extracellular matrix proteins in human breast cancer cells and drives colon cancer invasion (8,9). While there is no report to show that this channel is expressed in HMCs, neural Na^+ channel, $Na_v1.6$, was found in melanoma cells. $Na_v1.6$ participates in the control of podosome and invadopodia formation and regulates cellular invasion in these cells (10). It is still unclear whether Na^+ channels affect cellular behavior by altering Ca^{2+} homeostasis.

As Ca^{2+} uptake and release are significantly increased during the action potentials (APs) in cardiac myocytes, we assume that Na^+ channels together with other channels participate in the formation of APs depolarization phase and increase Ca^{2+} influx and efflux in HMC and melanoma cells. Studies have indicated that ultraviolet (UV) light induces APs in both HMC and melanoma cells. UV light depolarizes cell membrane through transient receptor potential A1 (TRPA1) channels, which can be blocked by a specific antagonist HC-030031. The increase of $[Ca^{2+}]_i$ occurs during depolarization phase of APs, and intracellular Ca^{2+} decays when the membrane is hyperpolarized (11-13). UV light activates a $G\alpha_q$/11-coupled phototransduction pathway in HMCs (12). However, the function of Na^+ channels in AP needs to be studied.

Here, we present a novel discovery that functional cardiac Na^+ channels, expressed in human melanoma cells (WM 266-4) but not in HMCs, depolarize the resting membrane potential (RMP) and decrease $[Ca^{2+}]_i$. Our research provides insights into the understanding of the molecular mechanism of the aggressiveness of melanoma cells which is related with Ca^{2+} homeostasis and may lead to novel clinical management of human melanoma like WM 266-4.

Materials and methods

Cell culture. Human skin melanocytes (ATCC® PCS-200-012™, Manassas, VA) were cultured in 254 medium (Life Technologies, Grand Island, NY, USA) with growth factor supplements. Human melanoma WM 266-4 cells were maintained in DMEM supplemented with 10% fetal bovine serum (FBS), penicillin/streptomycin (1:100; all Sigma, St. Louis, MO, USA) and 100 mM sodium pyruvate, in a CO_2 incubator at 37˚C.

Immunofluorescence staining and confocal microscopy. Cells were plated in 8-well chamber slides (Lab-Tek, Nalge Nunc International, Naperville, IL, USA) and washed in phosphate balanced saline (PBS) to remove traces of medium. The cells were then fixed for 20 min in fresh 4% paraformaldehyde-PBS, permeabilized and blocked with normal goat serum (diluted 1:10) for 2 h in PBS. Cells were then washed three times in PBS and incubated with primary antibodies, anti-$Na_v1.1$ (ASC-001), -$Na_v1.2$ (ASC-002), -$Na_v1.3$ (ASC-004), -$Na_v1.5$ (ASC-005) (14), and anti-$Na_v1.6$ (ASC-009) (15) from Alomone Labs (Jerusalem, Israel) 1:100, 1 h at room temperature. Those antibodies were recommended to be used in WB for human tissue, and also widely in immunofluorescence studies (14,15). The primary antibody incubation was followed by another three times PBS wash and incubation in secondary antibodies, Alexa Fluor® 594 goat anti-rabbit IgG (dilution in PBS 1:500) and Alexa Fluor® 488 goat anti-mouse IgG (dilution in PBS 1:500, green; Life Technologies) at room temperature for 1 h. The cell nuclei were also stained with Hoechst 33342 (1 μg/ml in PBS) for 10 min. The slides were mounted with anti-fade (Life Technologies) and kept in the dark until viewing. The samples were observed under a confocal microscope (Carl Zeiss AG, Oberkocken, Germany) and images were captured by Zen 2009 Light Edition.

Western blot analysis. Cells were cultured in 6-well plates, treated under respective treatments and then lysed using RIPA buffer. The lysates were then run through 10% SDS-PAGE. The gels were run through semi-dry transfer (Trans-blot SD Semi-dry Transfer Cell; Bio-Rad, Hercules, CA, USA) onto PVDF membranes. Membranes were blotted with primary antibodies 4°C over night. Anti-Nav1.1, -$Na_v1.2$, -$Na_v1.3$, -$Na_v1.5$, and anti-$Na_v1.6$ are from Alomone Labs (1:1,000). Secondary antibodies, IRDye® 680LT goat anti-mouse (dilution in PBS 1:10,000, red) and IRDye® 800CW goat anti-rabbit (1:10,000; LI-COR Biosciences, Lincoln, NE, USA). The secondary antibodies were incubated for 1 h at room temperature. Beta actin was used as a housekeeping control gene in western blotting. The proteins were then detected with Li-COR Odyssey imaging system.

Electrophysiological recordings. Perforated whole-cell current-clamp by an Axopatch-200B amplifier (Molecular Devices, Foster City, USA) was used to record APs at room temperature. The glass pipettes were filled with 120 mmol/l potassium gluconate, 20 mmol/l KCl, 5 mmol/l NaCl, 5 mmol/l HEPES, and 5 mmol/l MgATP (pH 7.2). The extracellular bathing solution (Tyrode solution) contained (in mmol/l) 140 mmol/l NaCl, 5.4 mmol/l KCl, 1 mmol/l $MgCl_2$, 10 mmol/l HEPES, 1.8 mmol/l $CaCl_2$, and 5.5 mmol/l glucose (pH 7.4). β-escin (50 μmol/l) was added to pipette solution. Pipette resistances were ~5 MΩ. Records were low-pass filtered at 10 kHz and digitized at 20 kHz. The exposure to 15 mJ/cm^2 UV light (280-320 nm) with duration of 12s was applied to induce depolarization of cells (11-13).

Na^+ channel currents were measured by using the whole-cell patch-clamp technique in the voltage-clamp configuration at room temperature. Healthy and tightly attached cells, with excellent morphological appearance, were used in this experiment. To measure Na^+ channel currents, pipettes (1-2 MΩ) were filled with a pipette solution containing: 80 mmol/l CsCl, 80 mmol/l cesium aspartate, 11 mmol/l EGTA, 1 mmol/l $MgCl_2$, 1 mmol/l $CaCl_2$, 10 mmol/l HEPES, and 5 mmol/l Na_2ATP (adjusted to pH 7.4 with CsOH). The bath solution is Tyrode solution. The holding potential was -100 mV. A voltage step of 200 ms ranging from -80 to +60 mV with steps of 10 mV was applied to establish the presence of Na^+ channel currents. The peak current density was used to plot I-V curves. The holding potential was -120 mV for inactivation measurement. A voltage step of 400 ms ranging from -120 to +30 mV with steps of 10 mV was applied before the final voltage -20 mV with duration of 40 ms to elicit the inactivation of Na^+ currents. Low pass filter was set as 10 kHz and currents were sampled at a frequency of 20 kHz. Cell capacitance and series resistance (>80%) were compensated (16).

Intracellular $(Ca^{2+})_i$ measurement. Fluo-4 AM (2 μM; Thermo Fisher Scientific, Inc., Franklin, MA, USA) was load to cells for 20 min in Tyrode solution at room temperature. Then cells were washed out three times by Tyrode solution and followed by a 20 min de-esterification (17). Cells were transferred onto the stage of a real-time florescence microscope (Olympus IX81; Olympus Corp., Tokyo, Japan). The images (2,048 x 2,048 pixels) were acquired at a room temperature. Analysis of the signals was performed with the software MetaMorph (version 7.8.11.0, Nashville, TN, USA). Ca^{2+} transients are presented as background-subtracted normalized

fluorescence (F/Fo). Basal cytosolic $(Ca^{2+})_i$ in those cells was measured.

Statistics. Data are shown as the mean ± standard error. The t-test was employed for two groups statistical analysis. Bonferroni correction and analysis of variance were performed for multiple comparisons. $P<0.05$ was considered to indicate a statistically significant difference. SigmaPlot (version 11.0; Systat Software, Inc., San Jose, CA, USA) was used for statistical analysis.

Results

Expression of Na^+ channels in HMC and WM 266-4 cells. If Na^+ channel expression changes are to contribute to malignancy, their expression should differ between benign and malignant cells. Therefore, we compared the expression of various Na^+ channels between HMCs and melanoma cells (WM 266-4). $Na_v1.5$ is cardiac Na^+ channel. $Na_v1.4$ is expressed in skeletal muscle while $Na_v1.1$, $Na_v1.2$, $Na_v1.3$, and $Na_v1.6$ subtypes are found in central nerve system. $Na_v1.7$, $Na_v1.8$ and $Na_v1.9$ subtypes are peripheral neural Na^+ channels observed in dorsal root ganglion (18). We first investigated the expression of central neural Na^+ channels and cardiac Na^+ channels in both HMC and WM 266-4. Western blot analysis indicated that Na_v 1.5 was expressed in both HMC and WM 266-4, but much less pronouncedly in HMCs. $Na_v1.6$ subtype was not observed in either HMC or WM 266-4 (Fig. 1A). Neither was $Na_v1.1$, $Na_v1.2$, $Na_v1.3$ (data not shown). Confocal microscopy results confirmed that only $Na_v1.5$ was expressed in both HMC and WM 266-4. The fluorescence intensity of $Na_v1.5$ was almost evenly distributed in the whole cell except the area of the nucleus (Fig. 1B). Two different secondary antibodies for actin in Western and Immunofluorescence from two different sources were used. In western blot, actin is red [Goat anti-Mouse IgG (H+L) Highly Cross-Adsorbed Secondary Antibody, Alexa Fluor Plus 488; cat. no. A32723], and in Immunofluorescence, actin is green (Alexa Fluor® 488 goat anti-mouse IgG). In Immunofluorescence or Confocal, those cells are derived from pigment cells which have numerous vesicles. Therefore, those actin-coated granules are likely melanosomes.

Cardiac Na^+ currents recorded in WM 266-4 cells. Then, we performed patch-clamp technique to measure Na^+ currents. The results showed that there was no Na^+ current recorded in HMCs. The maximum current density of Na^+ channels obtained in WM 266-4 was 1.7±0.3 pA/pF at -10 mV (Fig. 2A and B). There was a tiny window of Na^+ current from -60 to -20 mV (Fig. 2C). Na^+ currents recorded could be partially blocked (by 23.1±2.8%) by 3 μM of tetrodotoxin (TTX) and almost totally blocked by 30 μM TTX in WM 266-4, while 300 nM TTX almost had no effect on Na^+ currents in WM 266-4 (Fig. 2A and D). This suggests that $Na_v1.5$ play a predominant role in Na^+ currents in WM 266-4.

APs recorded in HMC and WM 266-4. Interestingly, melanoma cells had depolarized RMPs of -50.5±2.7 mV, which would be expected to generate a cardiac Na^+ channel window current (Fig. 2C). The RMP could be significantly hyperpolarized by 30 μM TTX. UV light, at 15 mJ/cm^2 (280-320 nm) with duration of 12s, could induce similar APs in both HMC and WM 266-4 (Fig. 3A and Table I). There was no significant difference in kinetic parameters (i.e., activation time constant and inactivation time constant of APs). The amplitudes of APs in WM 266-4 were slightly smaller than those in HMC. TTX, 30 μM, could partially increase the AP amplitude, time constants and prominently hyperpolarize RMP in WM 266-4 (Table I). AP recorded from HMCs was totally abolished by TRPA1 specific blocker, 100 μM HC-030031 (Fig. 3B). This suggests that the contribution of Na^+ channels to APs is very limited.

The cytoplasmic Ca^{2+} images in both HMC and WM 266-4. One possibility for how the presence of Na channels can affect malignancy is that they alter Ca^{2+} handling. Therefore, we measured cytoplasmic Ca^{2+} in both HMC and WM 266-4 cells. The results showed that the normalized fluorescence intensity (F/Fo) of HMC was significantly less than that in WM 266-4 (Fig. 4). Compared to WM 266-4 cells, HMCs had only 47% of the basal Ca^{2+}. In WM 266-4 cells but not HMCs, the normalized fluorescence intensity increased robustly from 7.2±0.6 to 11.2±0.9 after 30 μM TTX was applied into bath solution for 15 min (Fig. 5). This suggests that Na^+ channels are contributing to reduce Ca^{2+} entry in melanoma cells.

Discussion

It had been reported consistently that increase of $[Ca^{2+}]_i$ can enhance oncogene-induced tumorigenesis and metastasis. Intracellular $[Ca^{2+}]_i$ is related to cell proliferation because transition from G1 to S during mitosis depends on an increase of $[Ca^{2+}]_i$ in mammalian cells (6). Our data showed that WM 266-4 melanoma cells have a higher intracellular calcium concentration than that in normal human skin melanocytes, thus supporting the above notion.

However, existing publications about the relationship between RMP and oncogene-induced tumorigenesis and metastasis are inconsistent. It has been argued that enhanced expression of Ca^{2+}-activated K^+ channels during cell proliferation provides a positive-feedback mechanism with a result of long-term changes in $[Ca^{2+}]_i$ that are required for the G1-S transition in the cell cycle (5,6). There is a reverse linear correlation between $[Ca^{2+}]_i$ and membrane potential in the range from -100 to +50 mV. Thus, overexpression of K^+ channels could hyperpolarize membrane and increase Ca^{2+} influx driving force and lead to enhancement of $[Ca^{2+}]_i$ (5). On the contrary, if Kir4.1 is overexpressed, the hyperpolarized membrane potential could reduce tumor induction by two canonical oncogenes (19). Therefore, forced hyperpolarization is suggested to reduce tumor incidence.

In the present study, we found that the current density of cardiac Na^+ channels is small but sufficient to depolarize the cell membrane to voltages within the Na^+ channel window current. In WM 266-4 melanoma cells, RMP was -50±2.7 mV, which is in the voltage range of Na^+ channel window current, from -60 to -20 mV. The TTX experiments demonstrate that the Na^+ channel current contributes to the depolarization of WM 266-4 cells' RMP. When Na^+ channels were blocked, RMP is hyperpolarized.

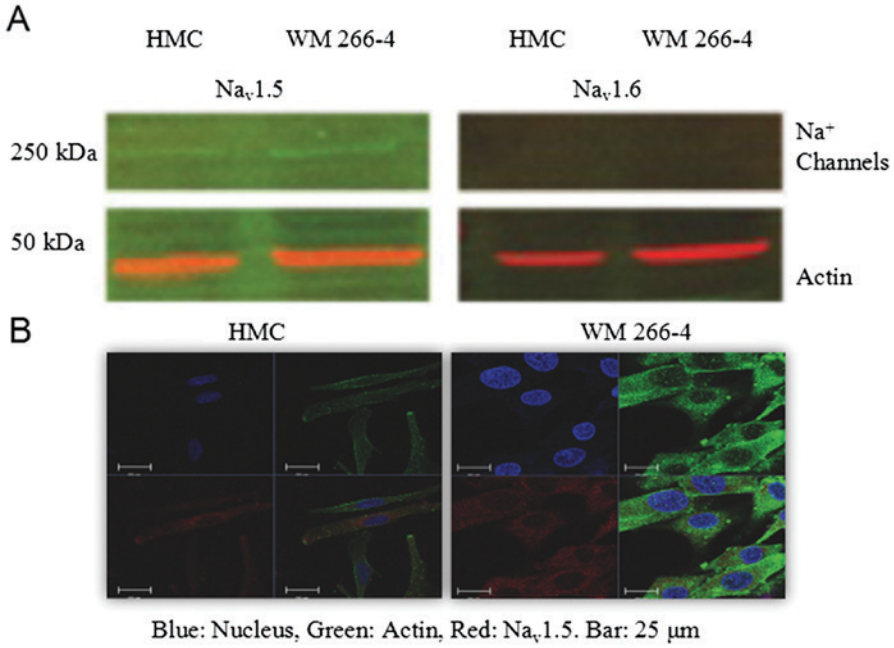

Figure 1. Expression of Na^+ channels in human skin melanocytes and melanoma cells. (A) HMC and melanoma cells (WM 266-4) were cultured in 6-well plates and cells were lysed for western blot analysis by using specific antibodies against Na^+ channel proteins. (B) HMC and WM 266-4 cells were cultured in eight well chamber slides and fixed and probed with antibodies against Na^+ channels, observed by confocal microscope. Scale bars, 25 μm. HMC, human skin melanocytes.

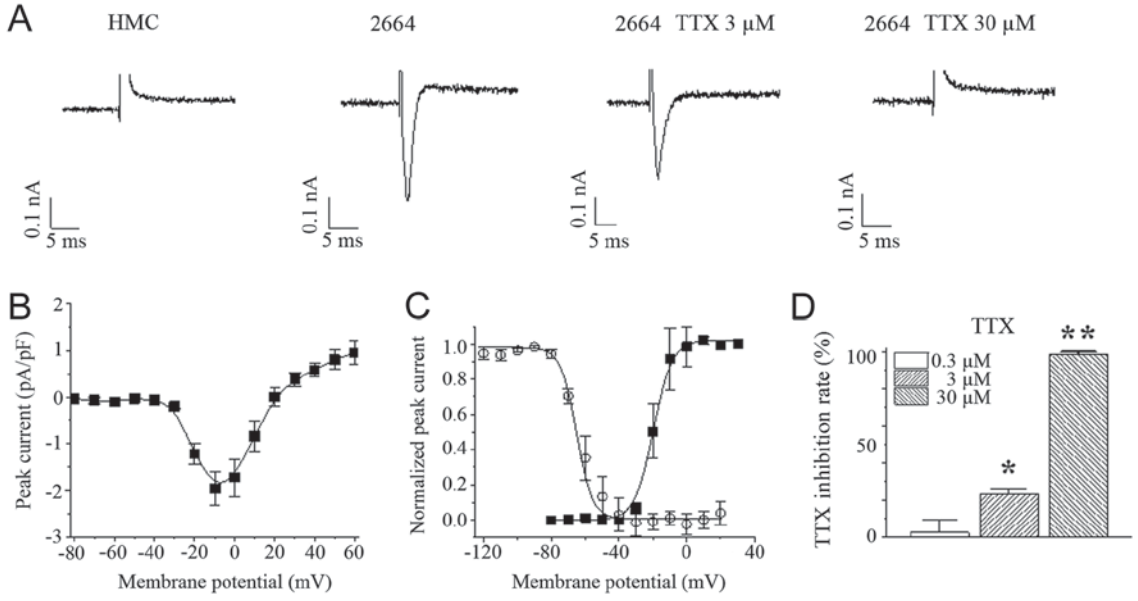

Figure 2. WM 266-4 cells show Na^+ currents while HMC cells are devoid of them. (A) The typical Na^+ currents recorded from HMC and WM 266-4 (w/o TTX) cells. The holding potential was -100 mV. A voltage step to -20 mV with duration of 200 ms was applied to record these Na^+ currents. The initial parts of Na^+ currents were plotted. (B) The average Na^+ currents I-V curve from eight MW 266-4 cells. (C) The average Na^+ currents activation (n=8) and inactivation curves (n=5). Data was fitted by Boltzmann function. (D) TTX concentration dependent inhibited Na^+ currents analyzed by ANOVA multiple comparisons. n=3 for each group. $^*P<0.05$ and $^{**}P<0.01$ vs. the 0.3 μM group. HMC, human skin melanocytes; TTX, tetrodotoxin.

Our experimental results then suggest that RMP determines the driving force for basal Ca^{2+} uptake. Ca^{2+} uptake through the membrane is voltage dependent by affecting the Ca^{2+} uptake driving force. In our case, it seems that cardiac Na^+ channel opening depolarizes the cell membrane and reduces Ca^{2+} uptake driving force. This would protect cells from Ca^{2+} overload. If Na^+ channels are blocked, RMP becomes more hyperpolarized, and Ca^{2+} is increased. This may result in the induction of tumorigenesis and metastasis.

The APs induced by UV light are assumed by inward Na^+ currents. But our experiment results prove that the induced APs are caused by TRPA1 channels. The APs induced by UV light in HMC and WM 266-4 cells are similar. These results suggest that the difference of $[Ca^{2+}]_i$ in HMC and WM 266-4 is determined by RMP, not the APs evoked by UV light.

Table I. APs evoked by UV light.

Group	RMP (mV)	APA (mV)	τ_{rise} (sec)	τ_{decay} (sec)	n
HMC	-70.3±4.1	9.7±1.1	8.8±1.7	28.2±12.5	9
WM 266-4	-50.5±2.7[a]	8.0±0.5	6.6±0.9	15.3±5.8	6
WM 266-4 + TTX	-61.0±2.9[b]	8.7±1.0	7.4±0.8	23.4±5.1	6

[a]P<0.01 vs. the HMC group. [b]P<0.05 vs. the WM 266-4 group. TTX was applied at 30 μM. RMP, resting membrane potential; AP, action potential; UV, ultraviolet; APA, amplitude of AP; τ_{rise}, the time constant of AP depolarization phase; τ_{decay}, the time constant of AP repolarization phase; HMC, human skin melanocytes; TTX, tetrodotoxin.

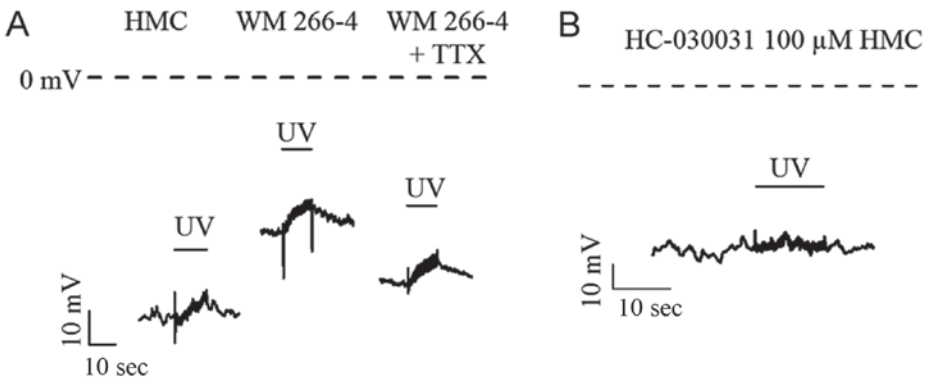

Figure 3. UV light induced APs in HMC and WM 266-4 cells. (A) APs induced by UV light in HMC and WM 266-4 cells (w/o 30 μM TTX). (B) A typical AP recorded from HMC was totally inhibited by, TRPA1 specific blocker, 100 μM HC-030031. The exposure to 15 mJ/cm^2 UV light (280-320 nm) with duration of 12 sec was applied to induce depolarization of cell membrane. Dash lines indicated 0 mV. HMC, human skin melanocytes; UV, ultraviolet; TTX, tetrodotoxin; AP, action potential.

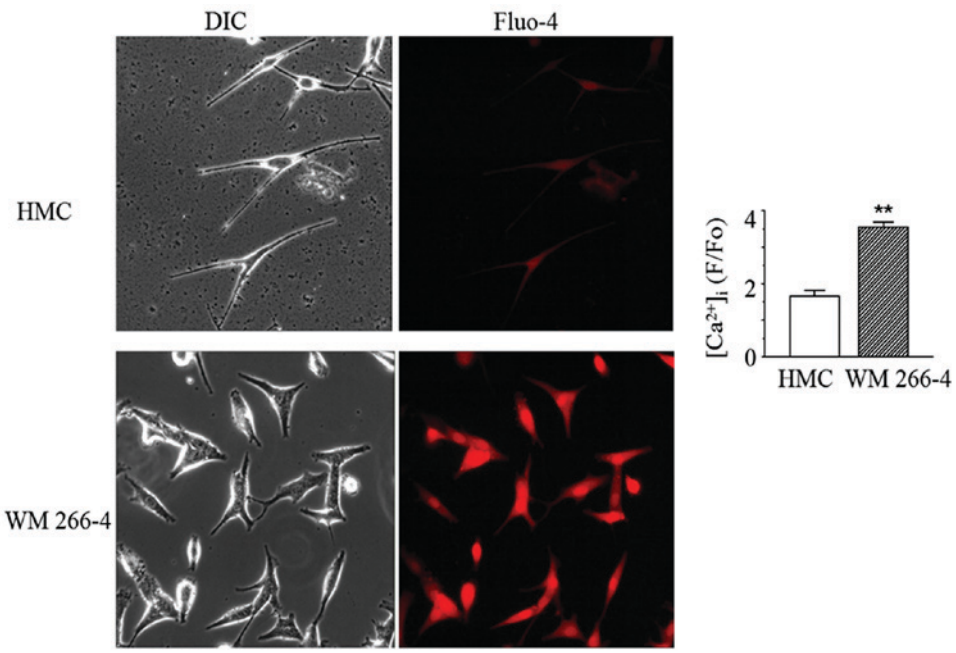

Figure 4. Cytoplasmic Ca^{2+} fluorescence images in HMC and WM 266-4 cells. Fluo-4 AM was load to HMC (n=5) and WM 266-4 (n=9) cells for 20 min in Tyrode solution at room temperature. Then cells were washed out three times by Tyrode solution and followed by a 20 min de-esterification. Cells were transferred onto the stage of a real-time florescence microscope. The images were acquired at a room temperature. Analysis of the signals was performed with the software MetaMorph. Ca^{2+} transients are presented as background-subtracted normalized fluorescence (magnification, x40). **P<0.01 vs. HMC. HMC, human skin melanocytes.

Na^+ channel-specific antagonist, TTX, is used as a therapeutic agent for cancer-related pain (20). The administration of TTX at doses below those that interfere with the generation and conduction of APs in normal (non-injured) nerves

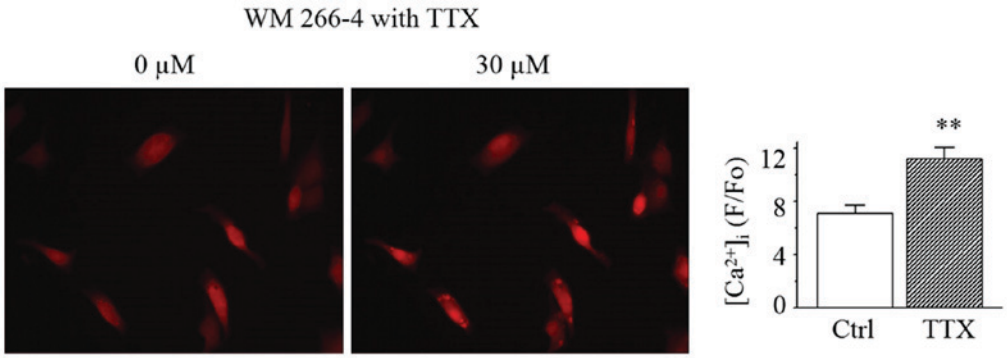

Figure 5. Alterations of cytoplasmic Ca^{2+} in WM 266-4 cells by 30 μM TTX. WM 266-4 cells (n=8) was pretreat with 30 μM of TTX compared with the un-treated group as control (n=8). Then cytoplasmic Ca^{2+} fluorescence images were acquired. Analysis of the signals was performed with the software MetaMorph. Ca^{2+} transients are presented as background-subtracted normalized fluorescence (magnification, x40). **P<0.01 vs. Ctrl. HMC, human skin melanocytes; TTX, tetrodotoxin; ctrl, control.

has been used in humans and experimental animals under different pain conditions. Nanomolar concentrations of TTX block $Na_v1.1$, $Na_v1.2$, $Na_v1.3$, $Na_v1.4$, $Na_v1.6$, and $Na_v1.7$ subtypes (TTX-sensitive Na^+ channel), whereas significantly higher (micromolar) concentrations are needed to block $Na_v1.5$, $Na_v1.8$ and $Na_v1.9$ subtypes (TTX-resistant Na^+ channel) (21). Therefore, there is no deleterious side effect on melanoma when nanomolar TTX is applied as a pain-killer. On the other hand, TTX is used to identify Na^+ channel subtypes (22,23). While $Na_v1.5$ had a median effective concentration of TTX at 5.7 μM, the median effective concentrations of TTX to $Na_v1.8$ and $Na_v1.9$ are 60 and 40 μM respectively (18). In our experiments, Na^+ currents recorded in WM 266-4 cells were almost completely blocked by 30 μM TTX and 300 nM TTX almost had no effect on Na^+ currents. This result suggests that almost all Na^+ currents recorded in WM 266-4 cells are from $Na_v1.5$.

We also performed test on another cell line, A375, using same culture conditions was also performed and results showed no Na^+ current. Melanoma cell lines are extremely heterogeneous, Studies showed that 40% of C8161 and C8146 cells have a voltage-activated Na+ channel, and SK28 and C832C do not have Na^+ channel as A375 cells we used (1). 100% of WM 266-4 cells have voltage-activated Na^+ channels and we had identified them as a Nav1.5 subtype. During patch clumping procedure, the test solution for both melanocytes and melanoma cells was the same. The recordings were similar. Thus we assume that culture medium we used is not a factor for channel expression, and tests on more cell lines should be performed in the future.

In conclusion, functional cardiac Na^+ channels are only expressed in WM 266-4 melanoma cells. Cardiac Na^+ currents depolarize cell membrane, reduce Ca^{2+} uptake driving force and have no relationship with UV light elicited APs that work through TRPA1 channels. WM 266-4 cells have an increased $[Ca^{2+}]_i$ which is suggested to facilitate tumorigenesis and metastasis. The blocking of cardiac Na^+ channels in WM 266-4 cells hyperpolarizes cell membrane and increases Ca^{2+} influx driving force and enhanced $[Ca^{2+}]_i$. Thus, cardiac Na^+ channels work to reduce melanoma cell proliferation and act as a protective function. In the meantime, cardiac Na^+ channel is a biomarker of carcinoma such as WM 266-4 melanoma as it can depolarize cell membrane. While further studies are still ongoing, this novel discovery provides insights into the understanding of the complex cellular and molecular mechanisms of the aggressive behavior of various forms of melanoma.

Acknowledgements

Not applicable.

Funding

This research project was supported by a grant from the National Institute of Health (grant no. P20RR016457; from the INBRE Program of the National Center for Research).

Availability of data and materials

The datasets used and/or analyzed during the current study are available from the corresponding author on reasonable request.

Authors' contributions

AX, HDC, YC and YW conceived and designed the study. AX, BG, HG, SCD, AG, MC, AM and FF performed research. AX, SCD and YW analyzed the data. AX and HG wrote the manuscript. AX, HG, YW, HDC, YC and SCD revised the manuscript.

Ethics approval and consent to participate

Not applicable.

Consent for publication

Not applicable.

Competing interests

The authors declare that they have no competing interests.

References

1. Allen DH, Lepple-Wienhues A and Cahalan MD: Ion channel phenotype of melanoma cell lines. J Membr Biol 155: 27-34, 1997.
2. Ekmehag B, Persson B, Rorsman P and Rorsman H: Demonstration of voltage-dependent and TTX-sensitive Na(+)-channels in human melanocytes. Pigment Cell Res 7: 333-338, 1994.
3. Zahradníková A, Zahradník I and Rýdlová K: Single-channel potassium currents in human melanoma cells. Gen Physiol Biophys 7: 109-112, 1988.
4. Lepple-Wienhues A, Berweck S, Böhmig M, Leo CP, Meyling B, Garbe C and Wiederholt M: K+ channels and the intracellular calcium signal in human melanoma cell proliferation. J Membr Biol 151: 149-157, 1996.
5. Nilius B and Wohlrab W: Potassium channels and regulation of proliferation of human melanoma cells. J Physiol 445: 537-548, 1992.
6. Nilius B, Schwarz G and Droogmans G: Control of intracellular calcium by membrane potential in human melanoma cells. Am J Physiol 265: C1501-C1510, 1993.
7. Das A, Pushparaj C, Bahí N, Sorolla A, Herreros J, Pamplona R, Vilella R, Matias-Guiu X, Martí RM and Cantí C: Functional expression of voltage-gated calcium channels in human melanoma. Pigment Cell Melanoma Res 25: 200-212, 2012.
8. Gillet L, Roger S, Besson P, Lecaille F, Gore J, Bougnoux P, Lalmanach G and Le Guennec JY: Voltage-gated sodium channel activity promotes cysteine cathepsin-dependent invasiveness and colony growth of human cancer cells. J Biol Chem 284: 8680-8691, 2009.
9. House CD, Vaske CJ, Schwartz AM, Obias V, Frank B, Luu T, Sarvazyan N, Irby R, Strausberg RL, Hales TG, *et al*: Voltage-gated Na+ channel SCN5A is a key regulator of a gene transcriptional network that controls colon cancer invasion. Cancer Res 70: 6957-6967, 2010.
10. Carrithers MD, Chatterjee G, Carrithers LM, Offoha R, Iheagwara U, Rahner C, Graham M and Waxman SG: Regulation of podosome formation in macrophages by a splice variant of the sodium channel SCN8A. J Biol Chem 284: 8114-8126, 2009.
11. Bellono NW, Kammel LG, Zimmerman AL and Oancea E: UV light phototransduction activates transient receptor potential A1 ion channels in human melanocytes. Proc Natl Acad Sci USA 110: 2383-2388, 2013.
12. Bellono NW, Najera JA and Oancea E: UV light activates a Gαq/11-coupled phototransduction pathway in human melanocytes. J Gen Physiol 143: 203-214, 2014.
13. Bellono NW and Oancea E: UV light phototransduction depolarizes human melanocytes. Channels (Austin) 7: 243-248, 2013.
14. Xu Q, Patel D, Zhang X and Veenstra RD: Changes in cardiac Nav1.5 expression, function, and acetylation by pan-histone deacetylase inhibitors. Am J Physiol Heart Circ Physiol 311: H1139-H1149, 2016.
15. Anderson LL, Hawkins NA, Thompson CH, Kearney JA and George AL Jr: Unexpected efficacy of a novel sodium channel modulator in dravet syndrome. Sci Rep 7: 1682, 2017.
16. Liu M, Sanyal S, Gao G, Gurung IS, Zhu X, Gaconnet G, Kerchner LJ, Shang LL, Huang CL, Grace A, *et al*: Cardiac Na+ current regulation by pyridine nucleotides. Circ Res 105: 737-745, 2009.
17. Mackenzie L, Bootman MD, Laine M, Berridge MJ, Thuring J, Holmes A, Li WH and Lipp P: The role of inositol 1,4,5-trisphosphate receptors in Ca(2+) signalling and the generation of arrhythmias in rat atrial myocytes. J Physiol 541: 395-409, 2002.
18. Lee CH and Ruben PC: Interaction between voltage-gated sodium channels and the neurotoxin, tetrodotoxin. Channels (Austin) 2: 407-412, 2008.
19. Lobikin M, Chernet B, Lobo D and Levin M: Resting potential, oncogene-induced tumorigenesis, and metastasis: The bioelectric basis of cancer in vivo. Phys Biol 9: 065002, 2012.
20. Hagen NA, Lapointe B, Ong-Lam M, Dubuc B, Walde D, Gagnon B, Love R, Goel R, Hawley P, Ngoc AH and du Souich P: A multicentre open-label safety and efficacy study of tetrodotoxin for cancer pain. Curr Oncol 18: e109-e116, 2011.
21. Nieto FR, Cobos EJ, Tejada MÁ, Sánchez-Fernández C, González-Cano R and Cendán CM: Tetrodotoxin (TTX) as a therapeutic agent for pain. Mar Drugs 10: 281-305, 2012.
22. Zhang YQ, Yang H, Sun WD, Wang J, Zhang BY, Shen YJ, Yin MQ, Liu YX, Liu C and Yun S: Ethanol extract of Ilex hainanensis Merr. exhibits anti-melanoma activity by induction of G1/S cell-cycle arrest and apoptosis. Chin J Integr Med 24: 47-55, 2018.
23. Yang H, Liu C, Zhang YQ, Ge LT, Chen J, Jia XQ, Gu RX, Sun Y and Sun WD: Ilexgenin A induces B16-F10 melanoma cell G1/S arrest in vitro and reduces tumor growth in vivo. Int Immunopharmacol 24: 423-431, 2015.